J Radioanal Nucl Chem (2013) 298:1137–1147
DOI 10.1007/s10967-013-2500-4

Synthesis of phosphorus-modified poly(styrene-co-divinylbenzene) chelating resin and its adsorption properties of uranium(VI)

Qiong Cao · Yaochi Liu · Xiu Kong · Lizi Zhou · Huijuan Guo

Received: 31 January 2013 / Published online: 9 April 2013
© Akadémiai Kiadó, Budapest, Hungary 2013

Abstract A new phosphorus-modified poly(styrene-co-divinylbenzene) chelating resin (PS–N–P) was synthesized by *P*,*P*-dichlorophenylphosphine oxide modified commercially available ammoniated polystyrene beads, and characterized by Fourier transform infrared spectroscopy and elemental analysis. The adsorption properties of PS–N–P toward U(VI) from aqueous solution were evaluated using batch adsorption method. The effects of the contact time, temperature, pH and initial uranium concentration on uranium(VI) uptake were investigated. The results show that the maximum adsorption capacity (97.60 mg/g) and the maximum adsorption rate (99.72 %) were observed at the pH 5.0 and 318 K with initial U(VI) concentration 100 mg/L and adsorbent dose 1 g/L. Adsorption equilibrium was achieved in approximately 4 h. Adsorption kinetics studied by pseudo second-order model stated that the adsorption was the rate-limiting step (chemisorption). U(VI) adsorption was found to barely decrease with the increase in ionic strength. Equilibrium data were best modeled by the Langmuir isotherm. The thermodynamic parameters such as ΔG_0, ΔH_0 and ΔS_0 were derived to predict the nature of adsorption. Adsorbed U(VI) ions on PS–N–P resin were desorbed effectively (about 99.39 %) by 5 % NaOH–10 % NaCl. The synthesized resin was suitable for repeated use.

Keywords Uranium · Phosphorus · Chelating resin · Synthesis · Adsorption

Q. Cao · Y. Liu (✉) · X. Kong · L. Zhou · H. Guo
College of Chemistry and Chemical Engineering, Central South University, Changsha 410083, China
e-mail: liuyaochi72@163.com

Introduction

The removal of uranium(VI) from the effluents of nuclear industry and related industries have received much attention in recent years. The toxic nature of the radionuclides, even at trace levels, has been a public health problem for many years [1, 2] According to World Health Organization guidelines and the US Environmental Protection Agency, the maximum concentration level of uranium in drinking waters has been regulated to be below 0.03 mg/L. The permissible discharge levels of uranium for industries range from 0.1 to 0.5 mg/L [3, 4]. Thus, precise estimation of uranium in the nuclear aqueous wastes is necessary and need to be separated prior to their final disposal.

The presence of long-lived radionuclides in water systems significantly increases the complexity and cost of treating the waste for disposal. Various removal methods of U(VI) from wastewater have been developed, such as chemical precipitation, membrane filtration, electrolytic methods, reverse osmosis, or solvent extraction [5]. However, these methods are not widely used because of their high cost and low feasibility for small-scale industries. In contrast, the adsorption [6–11] technique has been proved to be one of the effective, cost and versatile methods for U(VI) removal when combined with an appropriate desorption step to solve the problem of sludge disposal.

A variety of solid adsorbents have been used for U(VI) removal from aqueous solutions, such as chitosan, modified chitosan resins, cross linked poly 2,2-bisacrylamido acetic acid, phytic acid modified polyacrylamide–bentonite composite, chemically modified polyurethane foam and polymer grafted lignocelluloses [4, 12–16]. Particularly, chelating resins have received an enormous attention due to the remarkable simplicity and high efficiency [17, 18]. As is well-known, chelating resins with various ligands can

bond with metal ions and thus own a foreground since their integrated interactions involving ion-exchange, physic-sorption and chelation [19, 20]. The adsorption of metal ions from aqueous solution to adsorbents is usually controlled by the properties of the functional groups of the adsorbents [21, 22]. Chelating resins with O, N and S donor atoms have not shown satisfactory adsorption characteristics for uranium. Recent research suggests that the adsorbents containing P groups have exhibited superior adsorption characteristics, especially in view of the high adsorption rate, high adsorption capacity, and selectivity for U(VI), and can help to realize the quantitative recovery of uranium [23, 24].

In this work, a new phosphorus-modified poly(styrene-co-divinylbenzene) chelating resin was synthesized and characterized. The synthesized resin was used for extracting U(VI) from aqueous solutions in batch process. Experimental parameters, such as pH, initial concentration of uranium, contact time, temperature, competition ionic strength and the amounts of resin were studied and optimized. The adsorption equilibrium and kinetics of U(VI) on the chelating resin were also investigated in detail.

Materials and methods

Materials

Ammoniated polystyrene beads (PS–NH_2, 20-40 mesh) obtained from Chemical Factory of Nankai University (Nanjing, China). *P*,*P*-dichlorophenylphosphine oxide ($C_6H_5P(O)Cl_2$) was purchased from Mingye Technology Company Limited (Wuhan, China). Dimethylbenzene, ethanol, nitric acid, sodium Hydroxide, sodium chloride, U_3O_8 were used without further purification.

Synthesis of phosphorus-modified poly(styrene-co-divinylbenzene) chelating resin

Step 1 ammoniated polystyrene beads (PS–NH_2) were extracted with refluxing EtOH for 8 h, washed thoroughly with 0.1 M NaOH, distilled water, 0.1 M HCl and distilled water for five times until neutrality, followed by vacuum drying at 333 K for 48 h.

Step 2 the chemical anchoring of the PS–N–P resin was carried out by reacting PS–NH_2 with *P*-dichlorophenylphosphine oxide ($C_6H_5P(O)Cl_2$), followed by hydrolysis. Five grams of pretreated PS–NH_2 resin was reacted with an excess of $C_6H_5P(O)Cl_2$ (15 mL, 0.1 mol) and dimethylbenzene (100 mL) in a 250-mL flask equipped with a condenser, a mechanical agitator and a thermometer. The reaction mixture was stirred slowly (80 rpm) on an oil bath at 323 K for 12 h. The obtained polymer particles were purified from the excess reactants by repeated washing with ethanol and distilled water, and dried in vacuum at 333 K. The synthesis scheme for chemical anchoring of the resin is represented in Fig. 1.

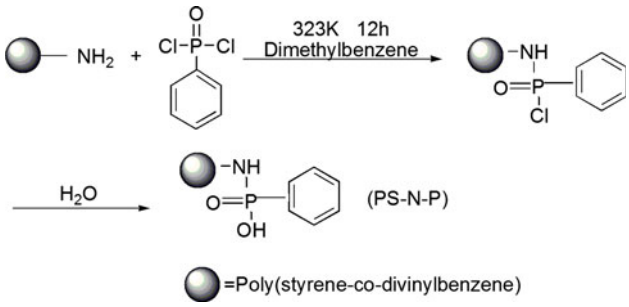

Fig. 1 Synthesis of phosphorus-modified poly(styrene-co-divinylbenzene) chelating resin

Equipments and methods of characterization

The resultant PS–N–P resin and ammoniated polystyrene beads were both characterized by Fourier transform infrared spectroscopy (FT-IR, Nicolet 170 SX) with testing conditions: potassium bromide pellets, scanning 32 times, resolution 1 cm^{-1}.

Element content changes of the resins were obtained using elemental analysis (EA, Elementar Vario MICRO).

The surface area and pore size distribution (ASAP 2020M+C) were detected by adsorption of nitrogen using the BET equation.

Adsorption of uranium

The removal of U(VI) from aqueous solution on resins was studied as a function of pH, contact time, adsorbent content and temperature. The concentration of U(VI) ions in aqueous solutions was measured using a UV–Visible spectrophotometer (UV759S). The initial pH of the sample solutions was adjusted by HNO_3 and NaOH, and measured using a pH meter (pHS-25). All of the mixtures were stirred (80 rpm) at different temperatures (278, 288, 298, 308 or 318 K).

The effect of pH

The effect of pH of the solution on the equilibrium uptake of U(VI) was studied over the pH range from 2.0 to 11.0. Pretreated resin (1 g/L) was added to U(VI) solution (100 mg/L) adjusted to desired pH.

Effect of contact time

Pretreated resin (1 g/L) was added to U(VI) solution (100 mg/L) adjusted to optimum pH 5.0. Samples were

taken at 0.5 h intervals for the analysis of residual U(VI) concentration in solution.

Effect of the resin amount

The effect of the resin amount was studied over the resin dose range from 0.25 g/L to 3 g/L, and with an initial U(VI) ion concentration 100 mg/L, at pH 5.0 and different temperatures.

Effect of the initial concentration of the U(VI) ion

The effect of initial concentration of the U(VI) ion on the uptake onto chelating resin was studied over initial concentrations range from 50 to 500 mg/L, and with an adsorbent dose of 1 g/L, at pH 5.0 and different temperatures.

Effect of competitive ions

Dried samples (1 g/L) of the chelating resins were added in mixed solution, including 100 mg/L U(VI) ion and 0 to 0.25 mol/L NaCl, adjusted to pH 5.0.

Samples were centrifuged at equilibrium and analyzed for the determination of the residual U(VI) concentration by UV. The uranium adsorption rate (removal percentage) and the quantities of metal ions adsorbed per unit mass of the resin were calculated as follows:

$$\text{Adsorption}\ (\%) = \frac{(C_0 - C_e)}{C_0} \times 100 \quad (1)$$

$$Q_e = \frac{(C_0 - C_e)\,V}{W} \quad (2)$$

Here, Q_e is the amount of uranium adsorbed at equilibrium (mg/g), C_0 is the initial uranium concentration (mg/L) and C_e is the equilibrium uranium concentration (mg/L), V is the volume of the system (L) and W is the amount of the resin used (g).

Dynamic adsorption

A glass column with an inside diameter of 30 mm and a length of 200 mm was packed with 10 g of PS–N–P resin. The resin (5 cm) was initially water treated followed by the passage of sample solution with a known metal concentration (100 mg/L) under optimum pH at the desired flow rate (1–4 mL/min).

Desorption of U(VI)

NaCl, NaOH and NaCl–NaOH solutions were employed as desorption medium. Pretreated resin (1 g/L) was added to U(VI) solution (100 mg/L) adjusted to optimum pH 5.0 for 5 h at room temperature. After the adsorption equilibrium, the resin was desorbed by added 100 mL various concentrations of NaCl, NaOH and NaCl–NaOH solutions at room temperature for one cycle, then, the desorbed resin was repeatedly used to the adsorption and desorption for further cycles.

The desorption percentage of U(VI) was calculated from the amount of U(VI) ion adsorbed on the resins and the final concentration of U(VI) ion in the desorption medium with the following equation:

$$\text{Desorption}(\%) = \frac{C_e^d V}{Q_e m} \times 100\ \% \quad (3)$$

where Q_e is the amount of uranium adsorbed at equilibrium (mg/g). m (g) is the mass of the adsorbents and V(L) is the volume of the system (L). C_e^d (mg/L) is the concentrations of U(VI) aqueous solutions after completely desorbed from the adsorbent.

Results and discussion

Characterization of chelating resins

The FT-IR spectra of modified chelating resin PS–N–P and ammoniated polystyrene beads were presented in Fig. 2. FT-IR spectra of both resins showed enhanced stretching vibrations at 2,923 cm^{-1} corresponding to –CH and $–CH_2$ groups. Appearance of characteristics band of NH stretching vibration group at 3,391 cm^{-1}, in addition to a band at 1,610 cm^{-1} due to NH bending vibration, suggested the presence of amine moiety on the resins. The spectrum of

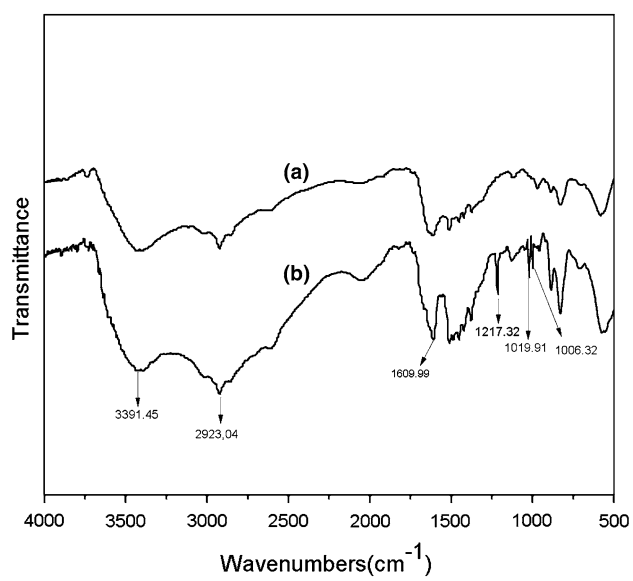

Fig. 2 FTIR spectra of ammoniated polystyrene beads (*a*) and modified chelating resin (*b*)

Table 1 Elemental analysis of ammoniated polystyrene beads and modified chelating resin

Elemental analysis (%)	Sample	
	PS–NH_2	PS–N–P
P	<0.01	0.21
C	81.21	85.35
H	7.717	4.421
N	5.015	3.225

PS–N–P showed a characteristic band at 1,217 cm^{-1} corresponding to the P=O group, and the bands at 1,019 and 1,006 cm^{-1} due to the P–OH stretching vibrations. In contrast, the spectra of PS–NH_2 resin didn't showed these characteristic peaks. These results demonstrated that a phosphorus-modified chelating resin was synthesized successfully by functionalizing ammoniated polystyrene beads with *P*,*P*-dichlorophenylphosphine oxide.

The results of P elemental analysis of resins were given in Table 1. The content of phosphorus for ammoniated polystyrene beads was less than 0.01 % and that of modified chelating resin was 0.21 %, which further confirmed the above-mentioned conclusion.

Adsorption–desorption isotherms of nitrogen at 77 K on both modified chelating resin and ammoniated polystyrene beads were carried out. The BET surface area of ammoniated polystyrene beads (193 cm^2/g) is larger than modified chelating resin (177 cm^2/g). Although ammoniated polystyrene beads is grafted with *P*,*P*-dichlorophenylphosphine oxide, the surface area of the modified chelating resin remains considerably high. This indicates that most of the pores with large diameters are not clogged with phosphorus functional groups, presumably because inner surface of the pores is uniformly covered with functional groups.

Uranium adsorption performance

Effect of pH and temperature

It is well known that the adsorption of heavy metal ions on resins is dependent on pH which extremely affects the chelation as well as physisorption processes. The effect of pH on the adsorption of U(VI) onto PS–NH_2 and PS–N–P was investigated in range of pH 2.0–11.0. Figure 3 shows the adsorption of U(VI) sharply increases with increasing pH from 2.0 to 5.0, and then decreases. Hence optimum pH 5.0 was used in all further studies. At pH 5.0, the maximum adsorption capacity of PS–NH_2 and PS–N–P resin for U(VI) are 38.28 and 97.60 mg/g, respectively. In addition, the fact that U(VI) adsorption is favoured at high temperature

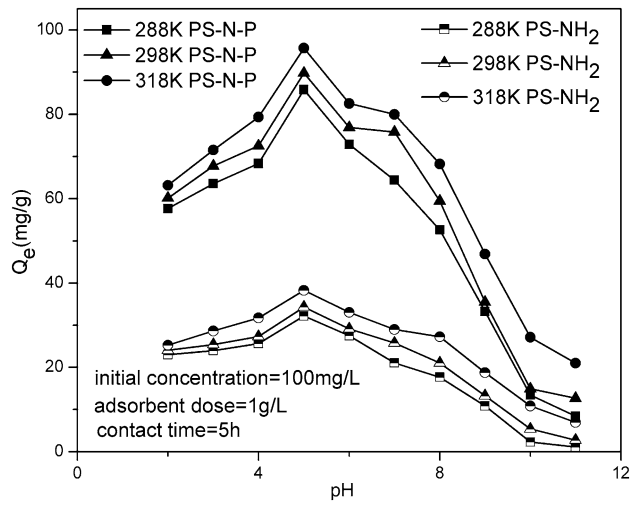

Fig. 3 Effect of pH on the adsorption of U(VI) onto PS–NH_2 and PS–N–P

indicates that the mobility of U(VI) ions increased with the rise of temperature, and hence it should interact efficiently with the adsorbent surface, i.e., the process is endothermic in nature.

According to Hu et al. [25], various hydroxo complexes of uranium may form when the pH increases from acidic value to the neutral value. The relative protonation of these species is determined by the pH and total uranium concentration. Repartition of the hydroxo complexes is determined by the following equilibria

$$UO_2^{2+} + 2H_2O \rightarrow UO_2(OH)^+ + H_3O^+ \quad (pK = 5.8) \tag{4}$$

$$2UO_2^{2+} + 4H_2O \rightarrow (UO_2)(OH)_2^{2+} + 2H_3O^+ \quad (pK = 5.62) \tag{5}$$

$$3UO_2^{2+} + 10H_2O \rightarrow (UO_2)_3(OH)_5^{+} + 5H_3O^+ \quad (pK = 15.63) \tag{6}$$

At the pH range 4.0–5.5, it is believed that ion exchange and complexation processes are major mechanisms for the removal of U(VI) ions [4]. Experimental data show that the pH at equilibrium is always less than initial pH. When the initial pH of solution varied between 3.0 and 5.5, the final pH of the reaction mixture remained between 2.5 and 4.3 for an initial concentration of 100 mg/L, respectively. The appearance of uranyl-hydrolysed species is favorable to metal ion adsorption. In the meantime, the modified chelating resin has –NH and O=P–OH groups, which make it suitable for complex formation with uranium. The nitrogen atom of –NH gets protonation at lower pH, and the phosphoric OH dissociates in the alkaline region, which would explain the decreasing adsorption of U(VI) with an increase in pH.

Effect of the resin amount

The adsorbent dosage is an important parameter because this determines the capacity of an adsorbent for a given initial concentration of the adsorbate. Effect of adsorbent dosage on the removal of U(VI) ion onto resins are shown in Fig. 4. The PS–N–P resin exhibited higher removal capacity. It was noticed that when the adsorbent dosage increased, the adsorption percentage of U(VI) improved as well. The adsorption of U(VI) achieved almost complete (>99 %) in a solution containing 100 mg/L U(VI) at 318 K for 5 h under 1.5 g/L adsorbent. The increase in the adsorption with the dose can be due to increased surface area and the availability of more adsorption sites, thus making easier penetration of the metal ion to the adsorption sites.

Effect of the initial concentration of the UO_2^{2+} ion

The results of the effect of initial U(VI) concentration on the uptake are shown in Fig. 5. The removal percentage of U(VI) ion decreased with the increasing of U(VI) initial concentration. This can be reasonably explained by the competitive adsorption occurs at higher initial concentration, because the adsorption sites are limited for a given amount of resin.

Adsorption kinetics

A study of adsorption kinetics is necessary for it provides information about the mechanism of adsorption. The adsorption kinetics of U(VI) onto PS–N–P at different temperature was studied in this part. The results are presented in Fig. 6. Adsorption equilibrium was attained in 4 h and was independent of temperature. The initial adsorption rate was high, and nearly 70–75 % adsorption capacity of U(VI) was achieved during the first 2 h, thenceforward, adsorption was gradual, and only 20–25 % additional removal percentage occurred in the subsequent 2 h. A further increase in contact time has a week effect on the adsorption efficiency after 4 h. With the increase of temperature from 278 to 318 K, the adsorption capacity increases from 77.83 to 89.42 mg/g.

It is well known that successful application of the adsorption not only need cheap, easily available and abundant adsorbents, but also demand innovation of known kinetic parameters. Adsorption kinetics can be studied by several models. The conventional pseudo first-order equation and

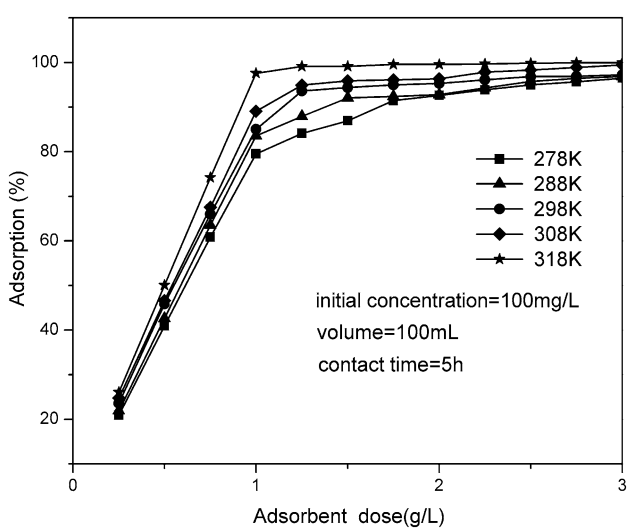

Fig. 4 Effect of the resin amount on the adsorption of U(VI) onto PS–N–P resin

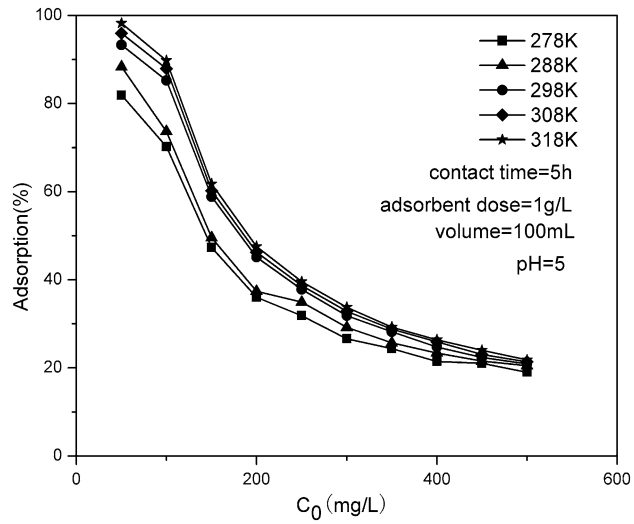

Fig. 5 Effect of the initial concentration of U(VI) on the adsorption of U(VI) onto phosphorus-modified chelating resin

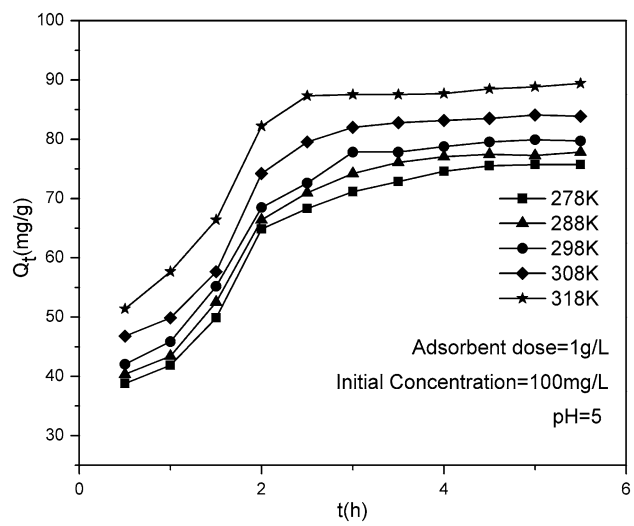

Fig. 6 Effect of contact time on the adsorption of U(VI) onto phosphorus-modified chelating resin

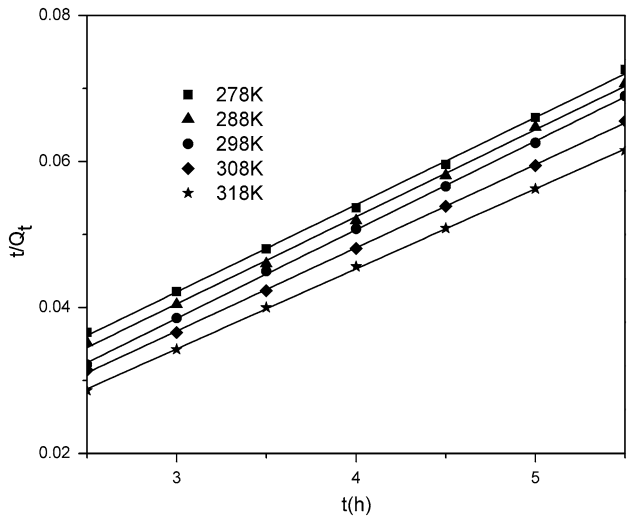

Fig. 7 Fitting results with the pseudo-second-order kinetics equation for U(VI) absorption at different temperatures

pseudo second-order rate equation given as follows (Eqs. 7 and 8) [26, 27] were firstly used to fit the experimental data, and the results are shown in Fig. 7.

$$\text{First - order model}: \ \log(Q_e - Q_t) = \log Q_e - \frac{k_1 t}{2.302} \tag{7}$$

$$\text{Second - order model}: \frac{t}{Q_t} = \frac{1}{k_2 Q_e^2} + \frac{t}{Q_e} \tag{8}$$

where $k_{1,2}$—adsorption rate constant (h^{-1} for first-order adsorption, g/mg/h for second-order adsorption), t—adsorption time (h), Q_e—the adsorption amount at equilibrium, Q_t—the adsorption amount at time t, h—original adsorption rate which can be defined as $h = k_2 Q_e^2$ (mg/g/h).

With an increase in temperature from 278 to 318 K, the rate constant k_2 increased from 0.02278 to 0.08284 g/mg/h while the initial adsorption rate (h) increased from 159.51 to 689.62 mg/g/h, indicating that the U(VI) adsorption on PS–N–P is an endothermic process. The correlation coefficients of linear plot were shown in Table 2, which stated that the adsorption was the rate-limiting step and the pseudo-second-order model is suitable to describe the experiment data. It is also found that the calculated adsorption amount at equilibrium (Q_e) are very close to the experimental values in the pseudo-second-order model. Hence, the rate limiting step may be chemisorption, which may involve valency forces through sharing or exchange of electrons between adsorbate and adsorbent.

The adsorption kinetic data are also tested whether the intraparticle diffusion is the rate-limiting step. The intraparticle diffusion kinetic model [28, 29] can be expressed as:

$$Q_t = k_{id} t^{0.5} \tag{9}$$

where k_{id} is the intraparticle diffusion rate constant (mg/g/h$^{-0.5}$), Q_t is the adsorption amount at time t. The values of k_{id} were calculated from the slope of the plot. The line of Q_t versus $t^{0.5}$ suggests the applicability of intraparticle diffusion controlling the kinetics of the adsorption. If the plots of Q_t versus $t^{0.5}$ were found to be linear and the high values of R^2 (0.8–0.9), it indicates that the intraparticle diffusion is the rate-determining step, and if the line does not pass through the origin, then intraparticle diffusion is not the rate-limiting step and the adsorption mechanism is quite complex [30].

The lines of intraparticle diffusion of U(VI) (Fig. 8) showed multilinearity with three different adsorption phases, including the external surface adsorption, the gradual adsorption stage which is due to intraparticle diffusion [31] and equilibrium stage. Moreover, the lines did pass through the origin. Hence, the results stated that the adsorption was the rate-limiting step and the pseudo-second-order model is suitable to describe the experiment data. For the pseudo-second-order reaction the rate limiting step may be chemisorption, which may involve valency forces through sharing or exchange of electrons between adsorbate and adsorbent.

As showed in Table 2, temperature has an important effect on the adsorption of U(VI), that is, the adsorption rate constant k increases with the increase of temperature. According to Arrhenius equation, $\ln k_2 = -E_a/RT + \ln A$, plotting $\ln k_2$ versus $1/T$, a straight line can be obtained. The apparent activation energy of adsorption Ea calculated from the linear slope is 25.46 kJ/mol. This low activation

Table 2 Pseudo-second-order kinetic parameters and intraparticle diffusion rate constants for the adsorption of U(VI) on PS–N–P resin

T (K)	Pseudo-second-order kinetics					Intraparticle diffusion	
	$Q_{e,exp}$ (mg/g)	R_2^2	k_2 (g/mg/h)	$Q_{e(cal)}$ (mg/g)	h (mg/g/h)	K_{id} (mg/g/h$^{-0.5}$)	R^2
278	77.83	0.99877	0.02278	83.68	159.51	24.12	0.80024
288	79.82	0.99841	0.03028	83.82	212.74	25.54	0.83414
298	83.92	0.99963	0.06218	87.72	478.46	25.45	0.83138
308	85.91	0.99961	0.07127	89.27	567.96	25.58	0.87020
318	89.42	0.99966	0.08284	91.24	689.62	25.30	0.88173

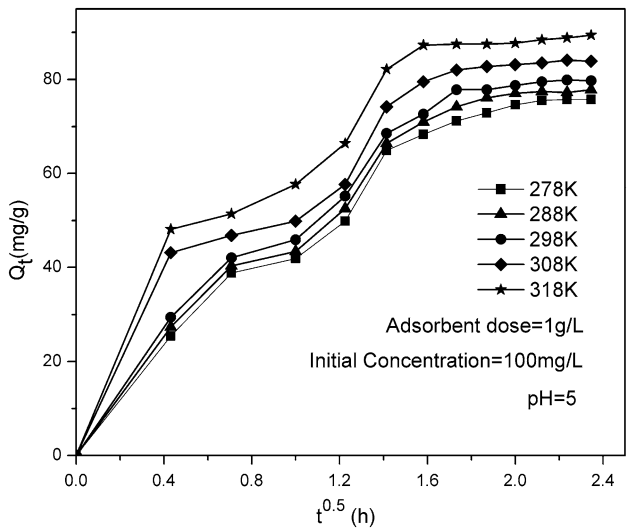

Fig. 8 Intraparticle diffusion plots for the adsorption of U(VI) onto PS–N–P at different temperatures

energy compared to these of typical chemical reaction of 65–250 kJ/mol implies that the adsorption of U(VI) on PS–N–P is a facile procedure. The thermodynamic parameters such as Gibbs energy (ΔG), enthalpy (ΔH), and entropy (ΔS) are calculated by the following equations [32].

$$K_c = \frac{Q_e}{C_e} \tag{10}$$

$$\Delta G = \Delta H - T\Delta S \tag{11}$$

$$\ln K_c = \frac{\Delta S}{R} - \frac{\Delta H}{RT} \tag{12}$$

where K_c is the thermodynamic equilibrium constant, T is the solution temperature (K), and R (8.3145 J/mol K) is the ideal gas constant. ΔH and ΔS are calculated from the slope and intercept of van't Hoff plots of log K_c versus $1/T$. The results are listed in Table 3. It can be seen that the adsorption process is spontaneous with the negative values of ΔG [33]. The positive value of ΔH justifies that the adsorption of U(VI) on PS–N–P is an endothermic process in nature. The ΔS being positive value shows an irregular increase of the randomness at the solid–solution interface during the adsorption of U(VI). This randomness state is mostly encountered in metal chelation due to the liberation of water molecules of chelation [34]. These thermodynamic data from adsorption experiments show that the negative values of ΔG at all temperatures indicating that the adsorption process is dominated by entropic rather than enthalpic changes [35].

Table 3 Thermodynamic parameters for U(VI) onto PS–N–P

T (K)	K_c(L/g)	ΔG (kJ/mol)	ΔH (kJ/mol)	ΔS (J/mol K)	E_a (kJ/mol)
278	5.128	−3.78			
288	5.181	−3.94			
298	7.143	−4.87	13.83	62.67	25.46
308	8.333	−5.43			
318	10.42	−6.20			

Adsorption isotherms

Adsorption isotherms are not only important in optimizing the use of adsorbent, but also describe how solute interacts with the adsorbent under equilibrium conditions. Isotherm studies give us some information about the capacity of the adsorbent to remove a unit mass of pollutant from wastewater. Adsorption isotherms of U(VI) at 278, 288, 298, 308 and 318 K were studied in batch experiments using different initial concentrations varying from 50 to 500 mg/L at pH 5.0 .

The adsorption data were fitted to two well known adsorption isotherm models of Langmuir (Eq. 13) and Freundlich type (Eq. 14), as shown in Figs. 9 and 10. The constants related to these isotherms have been given in Table 4.

$$\frac{C_e}{Q_e} = \frac{1}{bQ_0} + \frac{C_e}{Q_0} \tag{13}$$

$$\ln Q_e = \ln K_F + \frac{\ln C_e}{n} \tag{14}$$

where Q_0 is the saturated adsorption capacity (mg/g), b is an empirical parameter, Q_e is the amount of uranium adsorbed at equilibrium (mg/g), C_e is the equilibrium concentration (mg/L), n is the Freundlich constant, and K_F is the binding energy constant reflecting the affinity of the resin to metal ions.

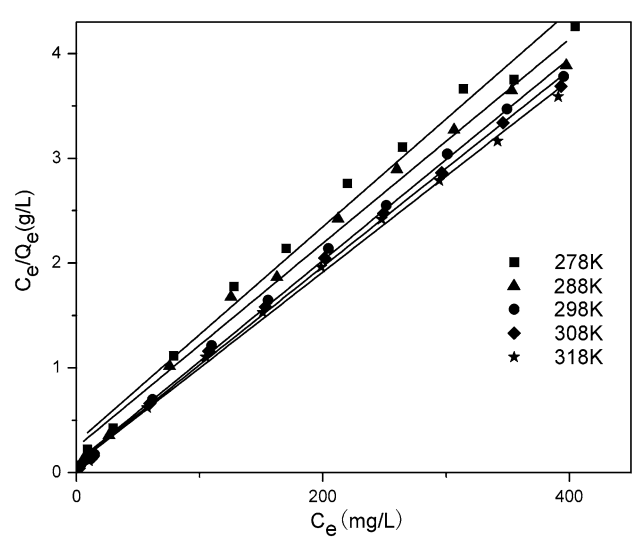

Fig. 9 Langmuir model fit toU(VI) onto modified chelating resin at different temperatures

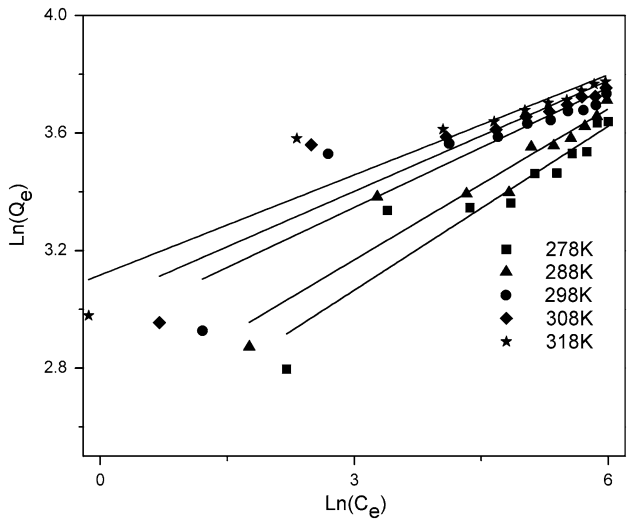

Fig. 10 The Freundich isotherms of PS–N–P for U(VI)

Table 4 Fitting results with Langmuir and Freundich model for U(VI) absorption by modified chelating resin

T (K)	Langmuir constants			Freundlich parameters		
	Q_0 (mg/g)	b (L/mg)	R^2	K_F	$1/n$	R^2
278	89.28	0.035	0.98515	12.26	0.1861	0.86797
288	93.78	0.040	0.98739	14.21	0.1714	0.90233
298	94.95	0.095	0.99733	18.88	0.1360	0.79448
308	96.51	0.10	0.99767	20.58	0.1256	0.81777
318	97.62	0.11	0.99740	22.57	0.1135	0.86539

Langmuir [36] adsorption isotherm assumes that the adsorbate molecules form an adsorbed layer with one molecule in thickness and that all sites are equal, resulting in equal energies and enthalpies of adsorption. While, the Freundlich equation is employed to describe heterogeneous systems and reversible adsorption, and it is not restricted to the formation of monolayer. In the present study, U(VI) was found to fit Langmuir type adsorption isotherm model better with higher correlation coefficient value ($R^2 > 0.98$). The adsorption isotherms data show that U(VI) adsorption increased with the increase in equilibrium concentrations. The higher temperature promotes the adsorption processes, which indicates the endothermic phenomena.

Effect of ionic strength and coexistent ions

As NaCl, KCl and KNO_3 are the main electrolytes present in nuclear fuel waters and environmental samples [37], their influences on the quantitative adsorption of U(VI) were studied.

The effect of ionic strength on uranium(VI) sorption was carried out with the resin dose 1 g/L, over NaCl concentrations range from 0 to 0.25 mol/L and U(VI) 100 mg/L. The results are shown in Fig. 11, U(VI) adsorption capacity decreased from 89.81 to 86.00 mg/g at 298 K, and there are similar trends under other temperatures, too. The decrease in the adsorption capacity is due to the decrease in contact area per unit mass of adsorbent, which makes harder penetration of the metal ion to the adsorption sites. Higher ionic strength creates a shielding effect on U(VI) ions at the PS–N–P surface causing a reduction in adsorption. But it is noticeable that, as shown in Fig. 11, the strong ionic strength had small influence on the adsorption of U(VI) onto PS–N–P, which further confirmed the higher affinity of PS–N–P toward U(VI).

The effect of coexistent ions containing K^+, Na^+, Ca^{2+}, Mg^{2+}, Fe^{3+}, CO_3^{2-}, Cl^-, NO_3^- on the uranium(VI) adsorption in PS–N–P at 298 K was investigated. The concentrations of these coexistent ions were adjusted to be several times of the uranium(VI). Table 5 shows that both cations and anions barely affect the uranium(VI)

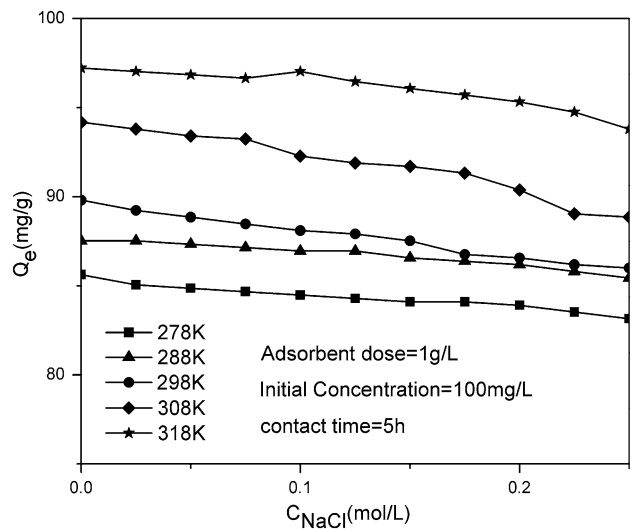

Fig. 11 Effect of competition ionic strength on the adsorption of U(VI) onto phosphorus-modified chelating resin at pH 5.0

Table 5 Uranium(VI) adsorption in the presence of coexistent ions

Ions	The concentration ratio[a]	Adsorption (%)
K^+	1,000	96.47
Na^+		97.82
Ca^{2+}	100	83.66
Mg^{2+}		87.68
Fe^{3+}	50	90.44
	100	82.11
	150	79.88
CO_3^{2-}	100	36.95
Cl^-	1,000	98.42
NO_3^-		97.93

[a] The concentration ratio of the foreign ions to the U(VI) ions

adsorption except CO_3^{2-}, which can be explained by larger complexation constants between uranium(VI) and CO_3^{2-}. All this characteristics of the synthesized adsorbent could be favorable for use in selective separation of uranium from nuclear industrial effluent.

Application

The applicability of the sorbent for adsorption of U(VI) was tested using synthetic seawater samples which was prepared according to the ref. [38] and the water of Xiang River (Changsha, Hunan, china). For the adsorption procedure, pH of the 1,000 mL of water samples was adjusted to 5 and spiked with uranyl ions and was subjected to the sorbent in batch methods. The sorbed U(VI) ions were estimated based on triplicate analysis (Table 6). It was found that the sorbent was successful in quantitative adsorption of the U(VI) ions even in the presence of various diverse ions.

Dynamic adsorption

The results of the effect of flow rate on the sorption are shown in Fig. 12. The results indicated that U(VI) adsorption on the resin was optimum at a low flow rate. The decrease with increasing flow rate in sorption is due to the decrease in equilibration time between two phases. The flow rates less than 1 mL/min were not studied to avoid long analyses times.

Desorption and regeneration

In order to improve its economic efficiency, it is necessary to study adsorption and desorption aspects of the process. In the present work, the desorption percentage of adsorption equilibrium phosphorus-modified chelating resin (1 g/L) was studied by various concentrations of NaCl, NaOH and NaCl–NaOH solutions at room temperature with batch experiments. Table 7 presents the desorption results and the adsorption–desorption cycles of U(VI) onto PS–N–P chelating resin. As shown in Table 7, the highest desorption percentage reached to nearly 100 % when 5 % NaOH–10 % NaCl solution were used as desorption agents, respectively. Therefore, 5 % NaOH–10 % NaCl was selected for the desorbent all further cycles. The results obtained on subsequent usage of the same resin showed the synthesized resin was suitable for repeated use without any noticeable loss of adsorption capacity, hence, the adsorbent PS–N–P can be economically used for the treatment of U(VI).

Table 6 Determination of U(VI) in water samples by the resin

Samples	Added C_0 (mg/L)	After adsorption C_e (mg/L)	Adsorption (%)
Synthetic seawater[a]	10	0.67	93.30
	10	0.98	90.20
	10	0.75	92.50
Xiang river	50	3.69	92.62
	50	4.46	91.08
	50	4.22	91.16

[a] Composition in *w/w* %; $Na^+ = 1.18$; $Cl^- = 2.2$; $Ca^{2+} = 0.005$; $K^+ = 0.04$; $Mg^{2+} = 0.15$

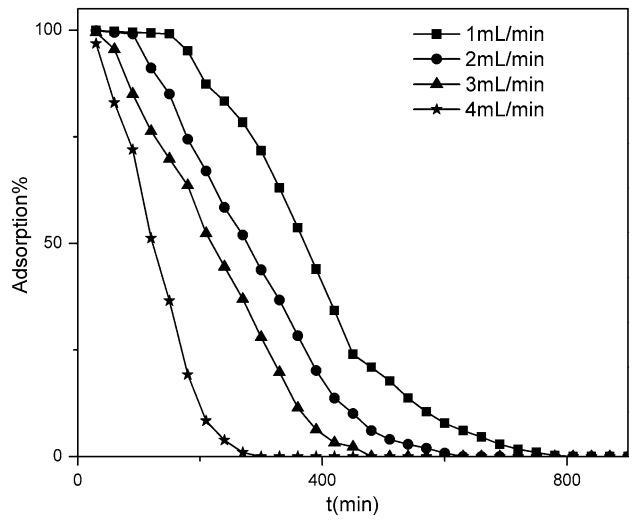

Fig. 12 Effect of flow rate on the adsorption of U(VI) onto PS–N–P chelating resin in a fixed bed ($C_0 = 100$ mg/L, inlet pH 5)

Table 7 Adsorption and desorption data

Cycle	Desorption agent	Equilibrium adsorption (%)	Desorption (%)
1	5 % NaCl	99.72	43.05
	10 % NaCl		72.33
	5 % NaOH		85.25
	10 % NaOH		89.12
	10 % NaCl + 2 % NaOH		96.47
	10 % NaCl + 5 % NaOH		99.39
2	10 % NaCl + 5 % NaOH	98.53	98.47
3		96.41	97.58
4		95.22	95.66

Conclusions

PS–N–P chelating resin was synthesized by *P*,*P*-dichlorophenylphosphine oxide modified commercially available ammoniated polystyrene beads. Through FT-IR and EA analysis, the phosphorus-containing groups were well

linked on ammoniated polystyrene beads. The obtained PS–N–P chelating resin has been demonstrated to be a very efficient adsorbent for the removal of U(VI) from aqueous solutions. The adsorption was found to be dependent on the solution pH, temperature and contact time. The maximum adsorption rate of U(VI) of 99.72 % occurs at 318 K and pH 5.0. The U(VI) adsorption capacity increased with contact time and attained equilibrium within 4 h, and decreased with the increase of ionic strength. The experimental kinetic data were analyzed using a second-order kinetic model. Equilibrium data were best modeled by the Langmuir isotherm. The uranium adsorbed on the synthesized resin was readily eluted (about 99.39 %) by 5 % NaOH–10 % NaCl.

Acknowledgments We acknowledge the Fundamental Research Funds for the Central Universities of Central South University (No. 2012zzts058) and the National Natural Science Foundation of China (No. 51074192) for financial support of this research.

References

1. Bozkurt SS, Cavas L, Merdivan M, Molu ZB (2011) Biosorption of uranium(VI) and thorium (IV) onto *Ulva gigantea* (Kützing) bliding: discussion of adsorption isotherms, kinetics and thermodynamic. J Radioanal Nucl Chem 288:867–874
2. Humelnicu D, Popovici E, Dvininov E, Mital C (2009) Study on the retention of uranyl ions on modified clays with titanium oxide. J Radioanal Nucl Chem 279:131–136
3. Anirudhan TS, Bringle CD, Rijith S (2010) Removal of uranium(VI) from aqueous solutions and nuclear industry effluents using humic acid-immobilized zirconium-pillared clay. J Environ Radioact 101:267–276
4. Anirudhan TS, Divya L, Suchithra PS (2009) Kinetic and equilibrium characterization of uranium(VI) adsorption onto carboxylate-functionalized poly(hydroxyethylmethacrylate)-grafted lignocellulosics. J Environ Manag 90:549–560
5. Girgin S, Acarkan N, Sirkeci AA (2002) The uranium(VI) extraction mechanism of D2EHPA–TOPO from a wet process phosphoric acid. J Radioanal Nucl Chem 251:263–271
6. Parsons JG, Iiemann KJ, Peralta-Videa JR, Gardea-Torresdey JL (2006) Sorption of uranyl cations onto inactivated cells of alfalfa biomass investigated using chemical modification, ICP-OES and XAS. Environ Sci Technol 40:4181–4188
7. Mahramanlioglu M (2003) Adsorption of uranium on adsorbents produced from used tires. J Radioanal Nucl Chem 256:99–105
8. Mahramanlioglu M, Bicer IO, Misirli T, Kilislioglu A (2007) Removal of uranium by the adsorbents produced from coffee residues. J Radioanal Nucl Chem 273:621–624
9. Jansson-Charrier M, Guibel E, Roussy J (1996) Dynamic removal of uranium by chitosan: influence of operating parameters. Water Sci Technol 34:169–177
10. Morsy AMA, Hussein AEM (2011) Adsorption of uranium from crude phosphoric acid using activated carbon. J Radioanal Nucl Chem 288:341–346
11. Bishay AF (2010) Environmental application of rice straw in energy production and potential adsorption of uranium and heavy metals. J Radioanal Nucl Chem 286:81–89
12. Atea AA (2005) Studies on the interaction of mercury(II) and uranyl(II) with modified chitosan resins. Hydrometallurgy 80:13–22
13. Rivas BL, Maturama HA, Ocampo X, Peric IM (1995) Adsorption behavior of Cu^{2+} and UO_2^{2+} ions on crosslinked poly [2,2-bis(acrylamido)acetic acid]. J Appl Polym Sci 58:2201–2205
14. Ulusoy U, Simsek S, Ceyhan O (2003) Investigations for modification of polyacrylamide–bentonite by phytic acid and its usability in Fe^{3+}, Zn^{2+} and UO_2^{2+} adsorption. Adsorption 9:165–175
15. El-Shahet MF, Moawed EA, Farag AB (2007) Chemical enrichment and separation of uranyl ions in aqueous media using novel polyurethane foam chemically grafted with different basic dyestuff sorbents. Talanta 71:236–241
16. Shukla SR, Pai RS, Shendarkar AD (2006) Adsorption of Ni(II), Zn(II) and Fe(II) on modified coir fibres. Sep Purif Technol 47:141–147
17. Wu FC, Tseng RL, Juang RS (2001) Kinetic modeling of liquid-phase adsorption of reactive dyes and metal ions on chitosan. Water Res 35:613–618
18. Shaw MJ, Nesterenko PN, Dicinoski GW, Haddad PR (2003) J. Chromatogr, Retention characteristics of lanthanide ions on a mixed phosphonic acid-carboxylic acid cation exchanger. Aust J Chem 56:201–206
19. Pramanik S, Dhara PK, Chattopadhyay P (2004) A resin containing bis(2-benzimidazo-lylmethyl)amine: synthesis and metal-ion uptake properties suitable for analytical application. Talanta 63:485–490
20. Stair JL, Holcombe JA (2007) Metal binding characterization and conformational studies using Raman microscopy of resin-bound poly(aspartic acid). Anal Chem 79:1999–2006
21. Yeom BY, Lee CS, Hwang TS (2009) A new hybrid ion exchanger: effect of system parameters on the adsorption of vanadium(V). J Hazard Mater 166:415–420
22. Zhou L, Wang Y, Liu Z, Huang Q (2009) Characteristics of equilibrium, kinetics studies for adsorption of Hg(II), Cu(II), and Ni(II) ions by thiourea-modified magnetic chitosan microspheres. J Hazard Mater 161:995–1002
23. Abderrahim O, Didi MA, Villemin D (2009) A new sorbent for uranium extraction: polyethyleniminephenylphosphonamidic acid. J Radioanal Nucl Chem 279:237–244
24. Wang P (2009) Carbon nanotubes using for recovery of radionuclides and separation of actinides and lanthanides. US 0093664 A1
25. Hu MZC, Norman JM, Faison BD, Reeves M (1996) Biosorption of uranium by Pseudomonas aeruginosa strain CSU: characterization and comparison studies. Biotechnol Bioeng 51:237–247
26. Ho YS, McKay G (1999) Pseudo-second order model for sorption processes. Process Biochem 34:451–465
27. Oliveira FM, Somera BF, Corazza MZ (2011) Cellulose microfiber functionalized with N,N′-bis (2-aminoethyl)-1,2-ethanediamine as a solid sorbent for the fast preconcentration of Cd(II) in flow system analysis. Talanta 85:2417–2424
28. Weber WJ, Morris JC, Sanit J (1963) Kinetics of adsorption on carbon from solution. J Sanit Eng Div Am Soc Civ Eng 89:31–60
29. Liu L, Li C, Bao C, Jia Q, Xiao P, Liu X, Zhang Q (2012) Preparation and characterization of chitosan/graphene oxide composites for the adsorption of Au(III) and Pd(II). Talanta 93:350–357
30. Kannan N, Meenakshisundaram M (2002) Adsorption of congo red on various activated carbons. Water Air Soil Pollut 138:289–305
31. Crank J (1979) The mathematics of diffusion. Carlendan Press, Oxford, London, pp 23–139
32. Tewari N, Vasudevan P, Guha BK (2005) Study on biosorption of Cr(VI) by *Mucor hiemalis*. Biochem Eng J 23:185–192
33. Subbaiah MV, Vijaya Y, Reddy AS, Yuvaraja G, Krishnaiah A (2011) Equilibrium, kinetic and thermodynamic studies on the biosorption of Cu(II) onto *Trametes versicolor* biomass. Desalination 276:310–316

34. Gode F, Pehlivan E (2003) A comparative study of two chelating ion-exchange resins for the removal of chromium(III) from aqueous solution. J Hazard Mater 100:231–243
35. Donia AM, Atia AA, El-Boraey H, Mabrouk DH (2006) Uptake studies of copper(II) on glycidyl methacrylate chelating resin containing Fe_2O_3 particles. Sep Purif Technol 49:64–70
36. Langmuir I (1918) The adsorption of gases on plane surfaces of glass, mica and platinum[J]. J Am Chem Soc 40:1361–1403
37. Raju SK, Subramanian MS (2007) Sequential separation of lanthanides, thorium and uranium using novel solid phase extraction method from high acidic nuclear wastes. J Hazard Mater 145:315–322
38. Spiegler KS (1962) Salt–water purification. Wiley, New York